Proceedings World Geothermal Congress 2020+1
Reykjavik, Iceland, April - October 2021

Geochemical Characterization of Geothermal Waters Circulation in Carbonate Geothermal Reservoirs of the Geneva Basin (GB)

Guglielmetti L.*, Eichinger F.**. Moscariello A.*,

*Department of Earth Sciences, University of Geneva. Rue des Maraichers 13, 1205 Genève (Switzerland)

**Hydroisotop GmbH. Woelksetr. 9, D-85301 Schweitenkirchen (Germany)

luca.guglielmetti@unige.ch

Keywords: Geothermal exploration, Geochemistry, Geothermal water, GEothermie2020, sedimentary basin

ABSTRACT

This study focuses on the interpretation of geochemical data collected at springs and at two deep geothermal exploration wells located on the edges and within the Geneva Basin (GB Canton of Geneva, Switzerland). The sampling sites have been selected across one North-South trending sections following the main groundwater flow from the recharge zone to the deep geothermal reservoirs in the Mesozoic carbonate units. These formations have been drilled by two geothermal exploration wells; the 745 m deep GEO-01 well, where water with a bottomhole temperature of 34˚C and an artesian flow rate of 50 l/s is encountered, and at the 2530 m deep Thonex-01 well, which produces app. 0.1 l/s by artesian flow at reservoir temperature of 80˚C. Major ions, trace elements, stable isotopes of Oxygen and Hydrogen, Tritium, Sulphur and Carbon isotopes as well as noble gas samples have been collected and analysed. The analyses aim at characterizing the fluid circulation in terms of recharge zone, origin of the water, mean residence times, reservoir temperature, and water-rock interactions. The interpretations show that the geothermal waters have a meteoric origin with the main recharge zone being located in the Jura Mountains towards the North. The infiltration is dominated by secondary porosity controlled by intense fracture conditions. Infiltrating water circulates in the Mesozoic units and the groundwater flow direction is controlled by the geometry of these formations, which gently dip towards south with a 3˚ average dip. Fracture zones associated to sub-vertical strike-slip faults represent the main corridors where waters as well as hydrocarbons and dissolved gas rise towards the surface. Moreover, the highly porous and permeable karstified horizons at the Lower Cretaceous level and the reef complex in the Upper Jurassic represent very promising potential geothermal reservoirs across the whole Geneva Canton for heat production with temperatures ranging from about 30˚C to more than 110˚C.

INTRODUCTION

The increased energy demand together with the political vision of reducing the use of fossil fuels for heat production in the Canton of Geneva triggered the development of medium to long term activities, in the framework of the Geothermie 2020 program (Moscariello, 2016). The program is driven by the Services Industriels de Genève (SIG), the Geological Survey of the Canton of Geneva (GESDEC) and is supported by national authorities such as the Swiss Federal Office of Energy (SFOE) and national research programs (i.e. the Swiss Competence Centre for Energy Resources (SCCER). This program aims at exploring and ultimately implementing geothermal energy focusing first on heat production and storage, and then on power production. The exploration activities carried out since now allowed identifying potential geological targets at shallow/medium (500-3000 m) to large depth (>3000 m) depths. to combine heat and power production.

The identification and characterization of geothermal resources is crucial to define potential geothermal developments. Geophysics, mostly 2D seismic has proved to be the most effective method to image the Mesozoic formations in the Geneva Basin (Clerc et al., 2015; Moscariello, 2016). However, the characterization of deep groundwater circulations has only been limited to the Thonex-01 well that was drilled in 1993, to tap fractured carbonates for heat production, reaching a depth of 2530m b.g.l. true vertical depth (TVD). Despite the favourable bottomhole temperature of 88˚C the extremely low flowrate of 3 l/s after stimulation in 1994 and 0.3 l/s artesian at present has proven to be unfavourable to proceed with a viable production (Jenny et al., 1995).

Only few geochemical studies on deep geothermal waters circulating in the Mesozoic units in the Geneva area have been carried out in the past. Muralt (1999) in his study compared several springs over the Molassic basin, covering for the Geneva area the only Thonex-01 well. In his study Muralt just few years after drilling and acidification operations were completed, constrained the meteoric origin of the waters which recharge zone is situated in the Jura Mountains, about 18-20km towards NW at an elevation of about 1000m was constrained. The water-rock interactions indicate a circulation in the Upper Jurassic limestone, giving a composition Na-Cl and a circulation time estimated to be 13’000 years according to Carbon isotopes. (Vuataz & Giroud, 2010) reported the results of geochemical analysis at the Thonex-01 well, carried out in 2010. These authors confirmed the origin and the recharge zone of the discharged waters, which are in thermal equilibrium with the reservoir at 2000-2500m in depth at an average temperature of about 85˚C. After about 15 years from the study of Muralt, Vuataz and Giroud also confirmed the residence time of about 10’000-15’000 years.

More recently, a study was carried out on the Thonex-01 well by (Sanjuan et al., 2016) in the framework of the FP7 IMAGE project. These authors focused on the development of auxiliary geothermometers (Na-Li, K-F, Na-Cs, K-Mn, Mg-Li, Na-Rb, K-Sr, K-Fe and K-W) confirming the reservoir temperature of 70±20˚C.

Chelle-Michou, et al., 2017 constrained the geothermal conditions over the Geneva Basin (GB) combining different sets of data from boreholes and exploration wells. In their study, the authors showed that the average geothermal gradient in the study area ranges between 25–30˚C/km, but areas of enhanced thermal regime could be located. South of Geneva, a positive thermal anomaly is recorded in the Humilly 2 well, most probably associated with up-flow of fluids from the Triassic units promoted by enhanced fracture conditions associated to the presence of fault corridors. The study identified the main target for geothermal energy in faulted and karstic reservoir in the Mesozoic units which, due to the potential high flow rate, can provide a solid geothermal resource for heat production. Electricity production, however, should target deeper reservoirs, in the Permo-Carboniferous troughs where the 140˚C temperature are expected at about 4000m in depth.

With this study, we aim to improve the understanding of the circulation of geothermal waters in the Geneva basin along a NW-SE section running from the main recharge zone where the Mesozoic units crop out in in the Jura Mountains towards NW, to the deep reservoirs towards SE, where the same units are located at depth and were drilled by the GEo-01 and Thonex-01 geothermal exploration wells.

The geometry, technical characteristics and schematic stratigraphy of the Thonex-01 well are shown in Figure 1. Water inflow with a temperature of 70˚C was observed in the Thonex-01 wells between 2110 and 2136 m TVD and with 80˚C at bottomhole at 2530m TVD.

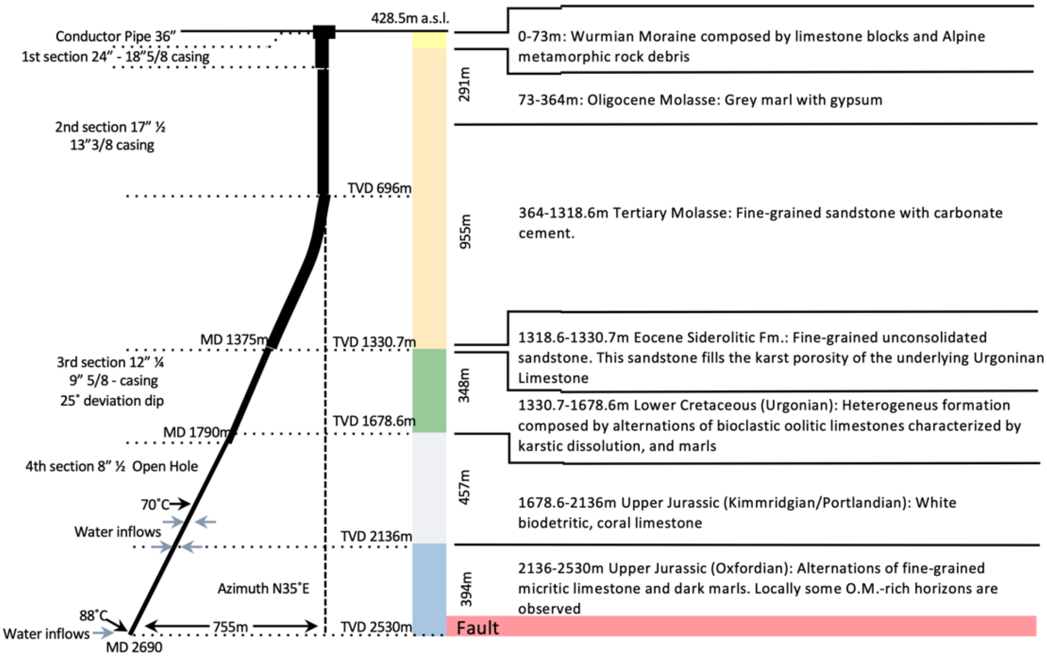

0-73m: Wurmian Moraine composed by limestone blocks and Alpine metamorphic rock debris

73-364m: Oligocene Molasse: Grey marl with gypsum

364-1318.6m Tertiary Molasse: Fine-grained sandstone with carbonate cement.

1318.6-1330.7m Eocene Siderolitic Fm.: Fine-grained unconsolidated sandstone. This sandstone fills the karst porosity of the underlying Urgoninan Limestone

1330.7-1678.6m Lower Cretaceous (Urgonian): Heterogeneus formation composed by alternations of bioclastic oolitic limestones characterized by karstic dissolution, and marls

1678.6-2136m Upper Jurassic (Kimmridgian/Portlandian): White biodetritic, coral limestone

2136-2530m Upper Jurassic (Oxfordian): Alternations of fine-grained micritic limestone and dark marls. Locally some O.M.-rich horizons are observed

Figure 1 - Thonex-01 well (modified from Jenny, 1995).

The geometry, technical characteristics and schematic stratigraphy of the GEo-01 well are shown in Figure 2. At GEo-01 well several water inflows (Table 1) were observed during drilling the open-hole section in the Mesozoic carbonates for a total flow rate of 55.6 l/s at 10 bars wellhead pressure and 34˚C wellhead temperature after drilling operation were completed.

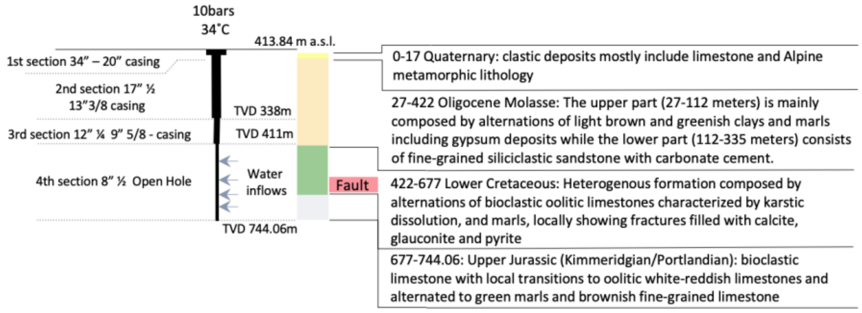

0-17 Quaternary: clastic deposits mostly include limestone and Alpine metamorphic lithology

27-422 Oligocene Molasse: The upper part (27-112 meters) is mainly composed by alternations of light brown and greenish clays and marls including gypsum deposits while the lower part (112-335 meters) consists of fine-grained siliciclastic sandstone with carbonate cement.

422-677 Lower Cretaceous: Heterogenous formation composed by alternations of bioclastic oolitic limestones characterized by karstic dissolution, and marls, locally showing fractures filled with calcite, glauconite and pyrite

677-744.06: Upper Jurassic (Kimmeridgian/Portlandian): bioclastic limestone with local transitions to oolitic white-reddish limestones and alternated to green marls and brownish fine-grained limestone

Figure 2 - GEo-01 well (modified from Nawratil de Bono, 2018).

Depth (meters TVD)	Total Flow rate (l/s)	Geologic Unit
455-486	3.9	Lower Cretaceous
522-537	8.3	
561-569	13.9	
611-628	16.1	
662-668	2.8	Upper Jurassic
692	2.8	
720-740	7.8	
TOTAL FLOW	*55.6*	

Table 1 – Productive fractures in the GEo-01 well (modified from Chablais, 2019)

GEOLOGIC SETTING

The Geneva Basin (GB) covers the western most part of the Alpine Molasse basin, including the Geneva Canton and the surrounding France. The GB covers an area of about 2000 km^2 extending from the town of Nyon to the NE, down to Vuache Mountain to the SW and it's limited by the Jura Haute-Chaine to the NW and by the subalpine nappes towards SE.

The GB consists of a thick sedimentary cover of Tertiary and Mesozoic age, principally composed of carbonates and marls overlying a crystalline basement often presenting tectonic depressions filled with Permo-Carboniferous clastic sediments (Signer & Gorin, 1995) as it was proved by the deep Humilly-2 well (Brentini, 2018; Meyer, 2000; Rusillon, 2018).

Based on the Humilly-2 and Thônex-01 wells stratigraphic record and the outcrops observations, the Geneva Basin, the Meso-Cenozoic sequence, from the top to the bottom, is summarized in Table 2.

Table 2 - Schematic stratigraphy if the geologic units in the Geneva Basin

Era	Period	Epoch	Lithology
Cenozoic	Quaternary		Heterogeneous, locally thick, glacial and fluvio-glacial and glacio-lacustrine sequences mostly genetically related to the last Würmian glaciation.
	Paleogene	Oligocene	In the GB area only the Lower Freshwater Molasse is observed in outcrops and borehole records and can reach a thickness of 1300m in the southern part of the region, where the Thônex-01 well is located (Guglielmetti et al. 2020).
Mesozoic	Cretaceous	Lower	Fine grained/bioclastic and fine quartz-rich bioturbated limestones alternating with organic-rich marls accumulated with a shallow and warm water environment. The top of the Lower Cretaceous is characterized by an erosive and highly karstified sequence boundary surface.
	Jurassic	Malm	Competent, often massive, shallow-marine platform carbonate deposits. locally the whole Malm interval could be highly fractured and karstified. Biothermal reefs facies are developed mainly during the Kimmeridgian-Thitonian interval and make this horizon a potentially interesting geothermal target where hot waters can circulate. The Purbeckian formation represents the last Jurassic stage and is more argillaceous than the underlying units.
		Dogger	Intercalations of marls and crinoidal limestone with quartz-detritic intervals toward the upper part.
		Lias	Bioclastic muddy limestones in the lower part and the organic-rich Posidonia shales as upper unit.
	Trias	Late	Succession of clastic, carbonates and evaporites overall reaching up to 500 m in thickness. The Triassic succession is typically capped by a shale unit known as the Rhaetian.
Paleozoic	Permian		Crystalline basement which only crops out in the Alps, southwards the GB. The basement is often affected by SW-NE oriented depressions (Moscariello et al., 2014; Moscariello, 2019) filled with several thousands of meters of Permo-Carboniferous sediments.
	Carboniferous		

The tectonic evolution of the GB is associated with the Alpine compressional phase that caused the decoupling of the sedimentary succession from the basement by a detachment surface occurring on the Triassic evaporites (Affolter & Gratier, 2004; Arn, Conrad, & Weidmann, 2005; Guellec, et al., 1990; Sommaruga, 1999). Additionally, inherited basement reliefs and normal faults bounding Permo-Carboniferous troughs might have played a role in the nucleation of the Mesozoic north-westward thrusts observed in the SE sector of the Geneva Basin and Bornes Plateau (Gorin, et al., 1993; Signer & Gorin, 1995).

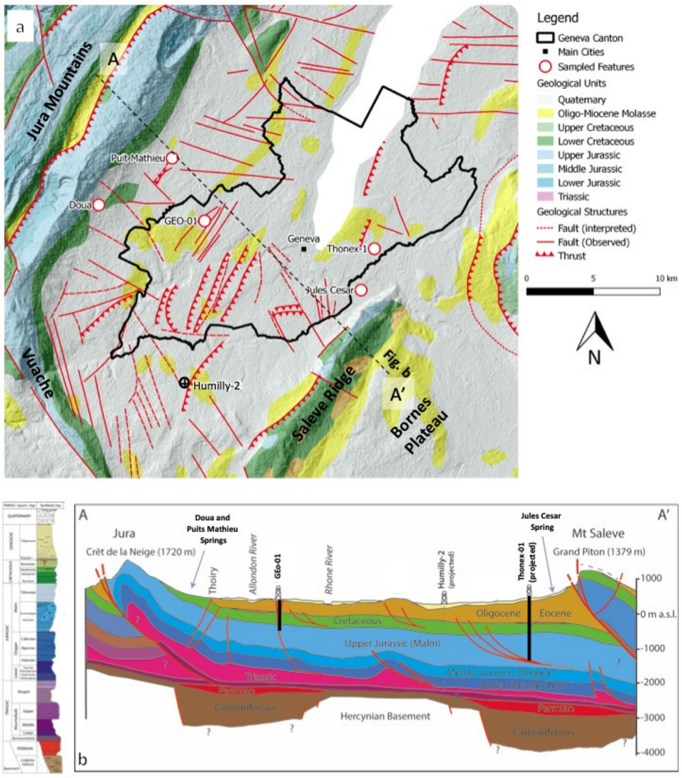

Figure 3 - a) Geological map over the Geneva Basin with indication of the main deep wells and sampled features (modified. from Brentini, 2018); B) Cross section cutting though the GB (modified from Moscariello et al., 2020)

METHODS

The company Hydroisotop GmbH was assigned by the University of Geneva to perform hydrochemical, isotopic and gas-physical analyses on water samples of five springs and two geothermal wells. The company Hydroisotop GmbH took samples from the springs, Source de Jules Cesar, Source de la Doua and Puits Matthieu as well as the wells GEO-01 and Thonex in the time of December 11 to 13, 2018. The location of the sampled figures is shown in Figure 3.

Sampling

The parameters temperature, pH, dissolved oxygen, specific electrical conductivity (EC) and redox value were measured in the field. Being very sensitive these parameters should be measured in flowing water. An adequate measurement was achieved by using a flow-through cell, which constantly renews the water inside and, hence, the water measured at the moment. A 10 litres bucket was used as a simple but functional flow-through cell.

Beside these parameters, alkalinity (acid capacity at pH 4.3) and the base capacity at pH 8.2 were determined in the field as well. As the carbonate content and equilibrium system are a major point for the characterization of the water chemistry, these parameters provide important onsite information. The determination is performed by titration using 0.1-mol HCl for the titration of alkalinity and 0.01-mol NaOH for the titration of the base capacity. The alkalinity-/ acid capacity complies with the amount of HCO_3^-, the base capacity with the dissolved CO_2, assuming that there is no main influence of contained organic acids on the titration.

Analysis

Measurements of the physic-chemical parameters pH, EC, and redox were done in the field using WTW probes. The determiantion of pH and EC, as well as the analysis of the alkalinity and acidity, which were carried out by titration, were repeated in the laboratory.

Main anions and cations were analysed by ionic chromatography using a Dionex ICS 1500 system. Trace elements and metals were determined using a Thermo Fischer ICP-MS system.

Stable water isotopes were determined by cavity ring-down spectroscopy using a Picarro L 2130-I Analyser. Tritium was analysed after electrolytic enrichment by liquid scintillation counting using a Perkin Elmer Quantulus 6220 low level liquid counter. More information about analytical methods can be found under www.hydroisotop.de.

RESULTS

The five sampled locations show water temperature ranging between 8.6˚C at Puit Mathieu spring to 32.4˚C at GEo-01 well, pH is between 7.1 (Jules Cesar Spring) and 7.7 (GEo-01 and Thonex-01 wells), the electrical conductivity ranges between 376 µS/cm (GEo-01 well) and 1789 µS/cm (Thonex-01 well). Interestingly, Jules Cesar spring shows rather high values (817 µS/cm). H_2S smell was perceived only at GEo-01 and Thonex-01 wells. In this study data have been interpreted using the free spreadsheet from Powell & Cumming, (2010).

Major Ions

Deep fluids circulating in carbonate aquifers such as those in the Cretaceous and Jurassic units in the study area, usually show geochemical facies dominated by Calcium (Ca) and Bicarbonate (HCO_3). However, fluids having deep and long paths (several kilometres), as well as a long residence time (thousands of years), show more complex geochemical composition due to the longer time and larger depth, hence temperature, which allow more complex water-rock chemical reactions. Additionally, such deep fluids flow towards the surface though fault corridors, where secondary minerals dominate the water-rock interactions during the last stages of the circulation. In sedimentary basins, where waters can reach several km in depth and temperature even above 100˚C, the main geochemical signature is dominated by Sodium (Na) and Chloride (Cl).

Both facies are observed in the Geneva area. The three springs show a clear $Ca-HCO_3$ composition even if the Jules Cesar Spring, shows a slightly higher temperature, a noticeable enrichment in $Na-Mg-Cl-SO_4-SiO_2$, a higher salinity, compared to the other two springs. GEo-01 well a predominant $Na>Ca- HCO_3$ and Thonex-01 well a predominant Na-Cl signature (Figure 4).

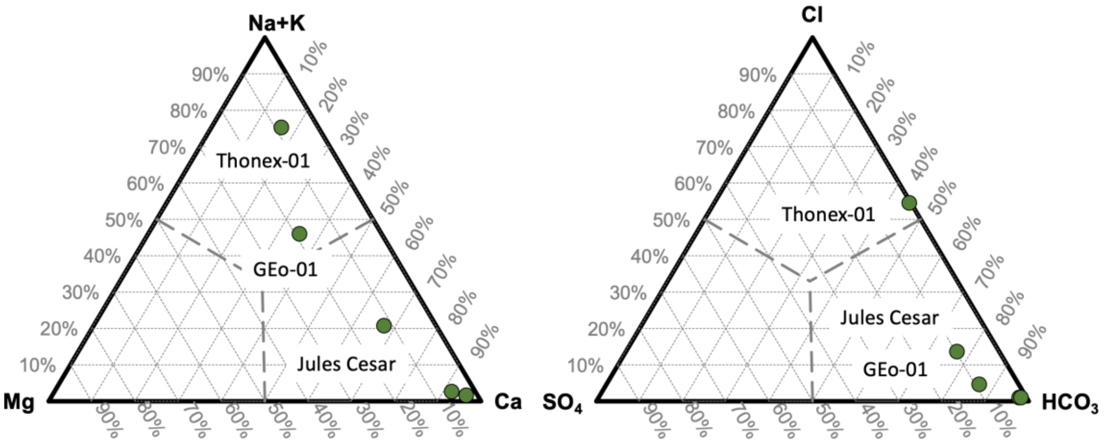

Figure 4: Ternary plots of the analysed samples.

Trace Elements

Trace elements have been analysed with particular focus on enhancing the differences between the springs and the wells.

The Thonex-01 wells show an enrichment in Br^-, NH_4^+ and Iron, whereas GEo-01 well shows concentrations similar to those from springs except for the Bromide which is higher.

Ammonia (NH_4^+) shows higher values in the two wells most probably associated to the presence of organic matter and hydrocarbons.

Cl/Br ratio observations were also carried out in this study, as it is an effective method to decipher the origin of the salinity. In fact values above 655 indicate halite dissolution, close to 655 is the value typical of seawaters, below 655 indicate that brines contribute to the Chloride content (Alcalá & Custodio, 2008; Sonney & Vuataz, 2010a). In this case, the analyzed waters show values between 4 (GEo-01) well and 600 (Jules Cesar Spring), suggesting that the circulating waters do not flow through any salt-rich formation, usually located in the Triassic Units, hence the circulation is limited to the Upper Mesozoic limestones.

GEOCHEMICAL INTERPRETATIONS

Chemical equilibria

Fluid-mineral equilibria were computed with PHREEQC (Parkhurst & Appelo, 1999) code choosing the most representative samples in terms of temperature and mineralization

Saturation Indexes for the Thonex-01 well were computed for the wellhead temperature of 14.3˚C and for increasing temperature up to the bottomhole temperature of 88˚C recorded after drilling operations (Jenny et al., 1995). The results are reported in Table 3.

All the spring and the GEo-01 well are in equilibrium with Calcite and undersaturated in Dolomite and evaporitic lithologies. With respect to Silica phases, all the springs are close to saturation with respect to Quartz. Thonex-01 well is slightly oversaturated in Calcite, Aragonite and Dolomite at both wellhead and bottomhole temperatures. This well is strongly undersaturated in gypsum and Anhydrite and at wellhead temperature it is in equilibrium with Chalcedony.

Table 3 – Saturation Indexes for selected minerals

	Saturation Index					
	Puits Matthieu	**Doua Spring**	**Jules Cesar Spring**	**GEo-01 Well**	**Thonex-01 Well (wellhead)**	**Thonex-01 Well (Reservoir at 90˚C)**
Temperature	8.6	9.5	12.1	32.4	14.6	88.0
pH	7.5	7.3	7.3	7.5	7.7	7.5
Calcite	-0.054	-0.073	-0.011	-0.072	0.346	0.944
Aragonite	-0.209	-0.229	-0.164	-0.215	0.191	0.836
Dolomite	-1.258	-1.695	-0.627	-0.075	0.514	1.931
Gypsum	-3.041	-3.025	-1.801	-2.611	-4.150	-4.162
Anhydrite	-3.534	-3.509	-2.252	-2.910	-4.626	-3.850
Amorphous Silica	-2.111	-1.818	-1.311	-1.255	-0.803	-1.366
Chalcedony	-1.213	-0.923	-0.426	-0.417	0.089	-0.702
Quartz	-0.730	-0.443	0.044	0.010	0.568	-0.435

Reservoir Temperature

The alkaline geothermometers of Na-K and Na-K-Ca with Mg correction were employed and compared to the other equations as it is demonstrated that the Na-K geothermometer, developed by Fournier, (1979) and (Giggenbach, 1988) highly overestimates the temperature for low enthalpy fluids (Sonney & Vuataz, 2010). At temperatures below 120˚C the sodium and potassium concentration are controlled by minerals such as clays and not only by the feldspar ion-exchange reactions which occur at higher temperatures (Nicholson, 1993).

To overcome this the Na-K-Ca geothermometer was developed by (Fournier & Truesdell, 1973) and later corrected by (Paces, 1975) to permit this equation to be reliably applied. The results shown in Table 4 show a good agreement between calculated and measured reservoir temperature for the GEo-01 and Thonex-01 well.

Table 4 – Reservoir temperature (˚C) estimated by Na-K-Ca and measured (n.a. = not applicable).

Sample Name	Na-K-Ca	Measured Temperature
Puits Matthieu	n.a.	8.6
Source de la Doua	n.a.	9.5
Source Jules Cesar	21	12.1
GEo-01 Well (wellhead)	36	32.4
GEo-01 Well (bottomhole)		34.0
Thonex-01 Well (wellhead)	84	14.6
Thonex-01 Well (bottomhole)		88

Origin of the fluid

The origin of thermal waters and elevation of the recharge zone can be estimated by means of the stable isotopes of hydrogen and oxygen. The results of the analysed samples for this study are compared to the world meteoric water composition (WMWC) and to the Swiss meteoric water composition (SMWC) by Kullin & Schmassmann, (1991), which slightly differentiates from the WMWC. The samples show δ^2H values between -82 δ‰ (Thonex-01 well) and -68.6 δ‰ (Jules Cesar Spring) and δ^{18}O values between -11.33 δ‰ (GEo-01 well) and-9.54 δ‰ (Jules Cesar Spring). All samples plot along meteoric lines, indicating a clear meteoric origin (Figure 5).

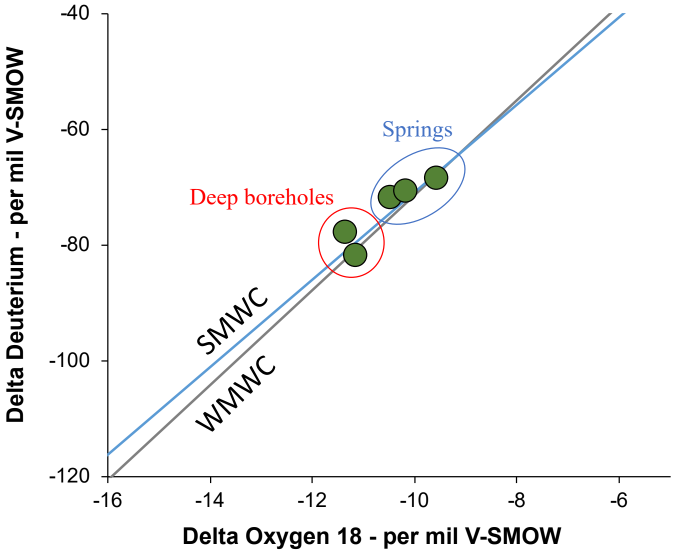

Figure 5: Stable isotopes of Oxygen and Hydrogen showing the meteoric origin of the sampled waters

To estimate the elevation of the recharge zone with the stable isotopes, hydrogen and oxygen can be used. Several equations have been developed for different regions based on the main assumption that the concentration in such isotopes remains constant with time. However, for very long residence times (>10’000 years), the results can be biased due to the infiltration in climatic conditions different from more recent times. Additionally, the δ^{18}O isotopic composition can be affected by isotopic fractioning. Therefore, δ^2H isotopes are considered as more reliable for elevation estimation. The equations used for this study are those for the Jura region (Blavoux, et al., 1979; Kullin & Schmassmann, 1991), Swiss Plateau (Blavoux, et al., 1979; Kullin & Schmassmann, 1991), Swiss Plateau (Kullin & Schmassmann, 1991), Swiss Plateau & Northern Alps (Vuataz, 1982) and Leman Prealps (Blavoux, 1978). Table 5 shows the results indicating an average recharge zone between 800 and 1400m, which is relatively coherent with the average elevation of the Jura Mountains. However, it has to observed that the results for the Geo-01 and Thonex-01 well are about 400-500m higher than those for the springs, suggesting that the recharge probably occurred in climatic conditions slightly different than at present (about 2˚C colder than now).

Table 5 – Recharge elevation estimation based on of δ^2H and δ^{18}O isotopes

	Puits Matthieu	Doua Spring	GEo-01 Well	Thonex-01 Well	Jules Cesar Spring	Authors	Isotope
Central Jura	1125	975	1565	1460	670	Kullin & Schmassmann, 1991	δ^{18}O
	957	878	1323	1561	744		δ^2H
French Jura & Swiss Central Jura	1017	850	1506	1389	511	Blavoux et al., 1979	δ^{18}O
	813	727	1213	1473	580		δ^2H
Swiss Plateau	625	518	939	864	300	Kullin & Schmassmann, 1991	δ^{18}O
	478	409	801	1011	290		δ^2H
Swiss Plateau & Northern Alps	728	618	1051	974	393	Vuataz, 1982	δ^{18}O
	661	601	936	1115	500		δ^2H
Leman Prealps (Thonon/Evian)	783	683	1077	1007	480	Blavoux, 1978	δ^{18}O
	680	628	920	1076	540		δ^2H

Residence Time

Groundwater residence time can be approached by means of Tritium, SF_6 and Carbon- 14 analyses. The spring waters have ^3H and SF_6 concentrations between 5.3 and 6.3 TU and between 3.0 and 3.7 fmol/L, respectively (Table 4). The modelling of the mean residence times using 75 % exponential and 25 % pistonflow model, which might reflect the investigated spring systems shows that the springs water consist of mainly young groundwater with residence times between 5 and 15 years (Figure 6).

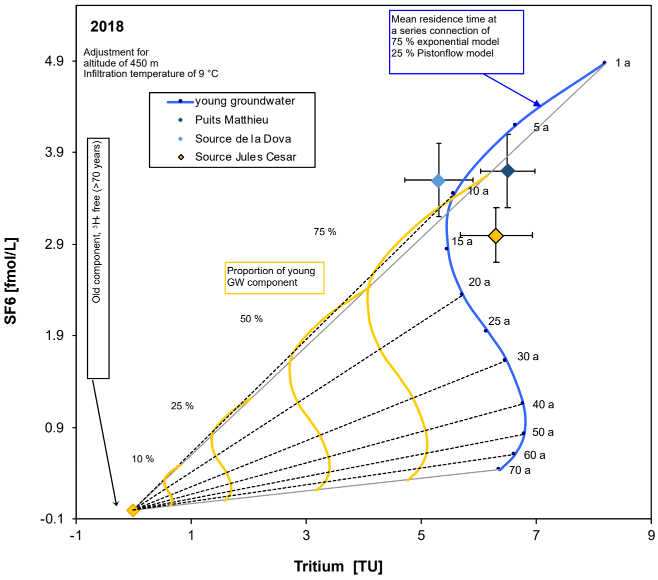

Figure 6 - Modelling of mean residence times of spring waters sampled in the Geneva Basin.

Tritium could not be detected in the groundwater sampled in the deep boreholes, indicating that there is no inflow of young water. Previous studies (Muralt 2000 and Vuataz & Giroud, 2010) determined a residence time between 10’000 and 15’000 years for Thonex-01 well using Carbon isotopes ($\delta^{13}C$=-2.3 ‰ PV-PDB and ^{14}C=2.2 pmC). These results are similar with those observed in 2018 for the Thonex well ($\delta^{13}C$ =-4.4pmC and ^{14}C=2.2 pmC). ^{13}C values decreased with respect to 2010 probably due to degassing, lowering pCO_2 during upflow, therefore enabling HCO_3 precipitation, making the $\delta^{13}C$ in the water lighter than in the reservoir rock where literature data report values of -0.2‰ V-PDB. Thermal water sampled in the GEo-01 borehole has a ^{14}C concentration of 18.01 pmC and a $d^{13}C$ isotope ratio of -4.4‰ V-PDB (Table 6) suggesting a shorter residence time than for the Thonex-01 well..

DISCUSSION

The sampled waters in this study show geochemical composition that reflects circulations within the Upper Mesozoic units which origin can be located between 800 and 1200m the Jura Mountains. The infiltration for the three springs occurred in recent times as confirmed by Tritium data, which also reveal a longer residence time for GEo-01 and Thonex-01 wells. If for the former well the residence is not at the moment fully constrained, previous studies on the Thonex-01 well estimated a residence time of 10’000-15’000 years.

The geochemical composition of the sampled features reveals that three main geochemical facies can be identified:

Puits Mathieu, and Doua springs show a classical $Ca\text{-}HCO_3$ composition dominated by water-rock interactions that occur during rapid circulation in the Mesozoic units as also confirmed by the equilibria with respect to the carbonate mineralogical phases.

Jules Cesar spring shows a dominant $Ca\text{-}HCO_3$ with higher temperature and concentrations in $Na\text{-}Cl\text{-}SO_4\text{-}SiO_2$ compared to the two other springs. This can be interpreted as partially related to anthropic pollution due road salt contamination but also to the result of mixing processes between two end-members which recharge zone from the Saleve ridge cannot be excluded: a recent (according to Tritium values) and shallow $Ca\text{-}HCO_3$ end-member and a deeper and slightly warmer $Na\text{-}Cl>SO_4$ end-member probably originating by leaching of deeper Mesozoic Units.

At GEo-01 the observed composition in $Na>Ca\text{-}HCO_3$ reflects a circulation within the Jurassic units, recharged in the Jura Mountains before the atmospheric nuclear tests (1953-1964). The waters discharged are in equilibrium with the carbonate mineralogical phases. The reservoir temperature estimated by the Na-K-Ca geothermometer is consistent with the one measured at the wellhead during the sampling campaign thanks to the large artesian flow observed. The discharged waters result from a mixing of relatively different water between different productive fractures in the Lower Cretaceous giving a pure $Ca\text{-}HCO_3$ composition and in the Upper Jurassic which can contribute to the Na, Mg concentrations. The presence of Mg rich end-member can be representative of the Oxfordian dolomite-rich lithologies which were not drilled by the GEo-01 well but that are most probably cut by fault structures that act as a preferential up-flow pathways towards the surface.

At the Thonex-01 well the Na-Cl geochemical imprint is correlated to long circulation both in terms of distance from the recharge zone and residence time. In fact, the waters discharging from the well are recharged by meteoric waters which infiltrated in the Jura Mountains in climatic conditions colder than at present and the residence time has been estimated to be between 10’000 and 15’000 years. During this time the infiltrated waters cover the distance of about 20km from the Jura Mountains to the well and have the time to get into full thermal equilibrium with the reservoir host-rock in the Jurassic formations. The Na-Cl composition results from Ca-Na ion exchange reaction that might occur at the Oxfordian formations which have been drilled in the last 400m of the well. This is also supported by the Magnesium concentration (higher than in the other sampled features, which can result from the water-rock interactions with dolomite-rich lithologies such as those in the Oxfordian.

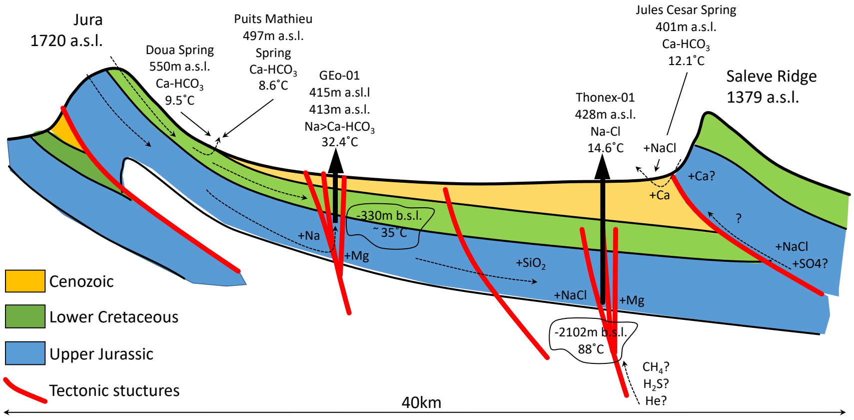

Figure 7: Conceptual model of groundwater circulation in the Geneva Basin (vertical and horizontal scales are not proportional).

CONCLUSION

In this study the results of the geochemical investigation on the liquid phase discharged from springs and two geothermal exploration wells are presented. The study focusses on the understanding the geochemical evolution of groundwater across a NW-SE oriented cross-section passing though the main infiltration zone of meteoric waters in the Jura Mountains towards NW, the Puits Mathieu and Doua springs located at the Jura foothills, the geothermal exploration wells GEo-01 drilled in 2018, and Thonex-01 drilled in 1993 and the Jules Cesar spring located at the SE of the section. All the analysed samples show a meteoric origin and the main recharge zone is located in the Jura Mountains. Only the Jules Cesar spring shows geochemical composition that can be most probably associated to an infiltration of meteoric waters at the Saleve Ridge and in part to anthropic contamination. The Puits Mathieu and Doua cold spring show the typical Ca-HCO$_3$ composition due to circulation in Lower Cretaceous, most probably controlled by karstic pathways allowing very rapid circulation as shown on Tritium data. The GEo-01 is 744m deep and discharges thermal waters at 32.4˚C with an artesian flow of 55.6 l/s and a wellhead pressure of 10bars. The geochemical composition of the discharged waters is most probably associated to a mix of pure Ca-HCO$_3$ groundwater from the Lower Cretaceous with a second endmember representative of water interacting with dolomite-rich lithologies such as those located at the base of the Upper Jurassic. The residence time of the water discharged by the GEo-01 well are not associated to recent and rapid circulations as shown by Tritium data, but Carbon isotopes reveal a residence time of probably some thousands of years. The Thonex-01 has been drilled to reach the Upper Jurassic reservoir at more than 2500m in depth. The bottomhole temperature recorded after drilling was 88˚C and residence times of more that 10'000 years have been estimated confirming previous analyses. The well discharge water at 14.6˚C having a Na-Cl geochemical composition due to the water-rock interactions that occur within the Upper Jurassic lithologies that compose the main reservoir. The Jules Cesar cold spring discharges a complex mix of waters most probably due to mixing processes between a cold, shallow and recent Ca-HCO$_3$ end-member and a deeper and warmer Na-Cl>SO$_4$ endmember. The results of this study highlight how deep circulation in the Geneva Basin have a common meteoric origin but complex circulations due to the heterogeneities i.e. in the reservoir rock in terms of mineralogical composition, tectonic setting and lithology. To further constrain the understanding of deep circulations in the Geneva Basin the study of the Carbon and Sulphur isotopes as well as the noble gases, hydrocarbon content will contribute reducing the uncertainty of the interpretation and providing new insights for future geothermal developments in the area.

AKNOWLEDGEMENTS

The authors would like to thank Services Industriels de Genève for funding this research and providing access to the well sites, and HydroGeo Environement Sarl for the fruitful support and dialogues in selecting the sampling sites.

This paper is also a contribution to the national Swiss research program SCCER SoE.

REFERENCES

Affolter, T., & Gratier, J.-P. (2004). Map view retrodeformation of an arcuate fold-and-thrust belt: The Jura case. *Journal of Geophysical Research*, *109*(B3). https://doi.org/10.1029/2002jb002270

Alcalá, F. J., & Custodio, E. (2008). Using the Cl/Br ratio as a tracer to identify the origin of salinity in aquifers in Spain and Portugal. *Journal of Hydrology*, *359*(1–2), 189–207. https://doi.org/10.1016/j.jhydrol.2008.06.028

Arn, R., Conrad, M. A., & Weidmann, M. (2005). *Nyon. Atlas géologique de la Suisse 1:25'000, feuille N° 117 and explanatory note*. Bern.

Blavoux. (1978). *Etude du cycle de l'eau au moyen de l'oxygène-18 et du tritium [Study of the water cycle using oxygen-18 and tritium]*. Université P et M Curie, Paris 6, France.

Blavoux, B., Burger, P., Chauve, P., & Mudry, J. (1979). Utilisation des isotopes du milieu à la prospection hydrogéologique de la chaîne karstique du Jura [Use of the isotopes for hydrogeological investigation in the karstic Jura range]. *Revue de Géologie*

Dynamique et Gèographique Physique, *21*, 295–306.

Brentini, M. (2018). *Impact d'une donnée géologique hétérogène dans la gestion des géo-ressources: analyse intégrée et valorisation de la stratigraphie à travers le bassin genevois (Suisse, France).* Terre & Environnement 140.

Chablais, J. (2019). Forage GEo-01 Satigny (Genève) GEothermie 2020 : Résultats du 1er forage de prospection à Satigny (OPS & hydrogéologie). *Proceed Journée Romande de Geothermie*. Lausanne.

Chelle-Michou, C., Do Couto, D., Moscariello, A., Renard, P., & Rusillon, E. (2017). Geothermal state of the deep Western Alpine Molasse Basin, France-Switzerland. *Geothermics*, *67*(2017), 48–65. https://doi.org/10.1016/j.geothermics.2017.01.004

Clerc, N., Rusillon, E., Moscariello, A., Renard, P., Paolacci, S., & Meyer, M. (2015). Detailed Structural and Reservoir Rock Typing Characterisation of the Greater Geneva Basin, Switzerland, for Geothermal Resource Assessment. *World Geothermal Congress 2015*, (April), 11. https://doi.org/10.1002/2017EF000724

Fournier, R.-O. (1979). A revised equation for the Na/K geothermometer. *Geothermal Resource Council Transactions*, 221–224.

Fournier, R.-O., & Truesdell, A. H. (1973). An empirical Na-K-Ca geothermometers for natural waters. *Geochimica et Cosmochimica Acta*, *37*(1255–1275).

Giggenbach, W.-F. (1988). Geothermal solute equilibria. Derivation of Na-K-Mg-Ca geoindicators. *Geochimica et Cosmochimica Acta*, *52*, 2749–2765.

Gorin, G., Signer, C., & Amberger, G. (1993). Structural configuration of the western Swiss Molasse Basin as defined by reflection seismic data. *Eclogae Geologicae Helvetiae*, *86*(3), 693–716.

Guellec, S., Mugnier, J.-L., Tardy, M., & Roure, F. (1990). Neogene evolution of the western Alpine foreland in the light of ECORS data and balanced cross-section. *Deep Structure of the Alps*, *156*, 165–184. Retrieved from http://cat.inist.fr/?aModele=afficheN&cpsidt=4341857

Guglielmetti, L., Poletto, F., Corubolo, P., Bitri, A., Dezayes, C., Farina, B.M., Martin, F., Meneghini, F., Moscariello, A., Nawratil de Bono, C., Schleifer, A. (2020). Results of a walk-above VSP survey acquired at the Thônex-01 Geothermal well (Switzerland) to delineate fractured carbonate formations for geothermal development. Geophysical Prospecting. In Press

Jenny, J., Burri, J. P., Mural, R., Pugin, A., Schegg, R., Ugemach, P., … R., W. (1995). Le forage geothermique de Thonex-01 (Canton de Geneve): Aspects stratigraphiques, tectoniques, diagenetiques, geophysiques et hydrogeologiques. *Eclogae Geologicae Helvetiae*, *88*(2), 265–396.

Kullin, M., & Schmassmann, H. (1991). Isotopic Composition of Modern Recharge. In FJ Pearson et al. Applied Isotope Hydrogeology. A Case Study in Northern Switzerland. In *Studies in Environmental Science* (Vol. 45, pp. 65–116).

Meyer, M. (2000). *Le Complexe récifal kimméridgien-tithonien du Jura méridional interne (France), évolution multifactorielle, stratigraphique et tectonique*. Thèse de doctorat: Univ. Genève, 2000 - Sc. 3170 – 2000.

Moscariello, A. (2016). Geothermal exploration in SW Switzerland. *European Geothermal Congress 2016, Strasbourg, France*, 9.

Moscariello, A., Guglielmetti, L., Omodeo-Salé, S., De Haller, A., Eruteya, O.-E., Lo, H.-Y., … Meyer, M. (2020). Heat production and storage in Western Switzerland: advances and challenges of intense multidisciplinary geothermal exploration activities, 8 years down the road. *World Geothermal Congress 2020*, submitted for publication. Reykjavik, Iceland.

Muralt, R. (1999). Processus hydrogéologiques et hydrochimiques dans les circulations profondes des calcaires du Malm de l'arc jurassien. (Verwendet in SGPK-Publikation Nr. 39). https://doi.org/Hydrovaud, PNR61, VD_3D, Synclinal_Delemont

Nawratil de Bono, C. (2018). GEo-01 : The first GEothermie 2020 P&D well in the Canton of Geneva - Preliminary results. *SCCER SoE Annual Conference 2018*. SCCER - Swiss Competence Center for Energy Research Supply of Electricity.

Nicholson, K. (1993). *Geothermal fluids: Chemistry and exploration techniques*. Springer Verlag.

Paces, T. (1975). A systematic deviation from Na-K-Ca geothermometer below 75 °C and above 10-4 atm PCO2. *Geochimica et Cosmochimica Acta*, *39*, 541–544.

Parkhurst, D.-L., & Appelo, C.-A.-J. (1999). *User's guide to PHREEQC (version 2) - a computer program for speciation, reaction-path, 1D-transport, and inverse geochemical calculations.*

Powell, T., & Cumming, W. (2010). Spreadsheets for geothermal water and gas chromatography. *PROCEEDINGS, Thirty-Fifth Workshop on Geothermal Reservoir Engineering*, unbekannt.

Rusillon, E. (2018). *Characterisation and Rock Typing of Deep Geothermal Reservoirs in the Greater Geneva Basin*. Terre & Environnement 141.

Sanjuan, B., Gal, F., Millot, R., Dezayes, C., Jirakova, V., Frydrych, V., … Hopm. (2016). *Final Report on chemical geothermometers and tracers*.

Signer, C., & Gorin, G. (1995). New geological observations between the Jura and the Alps in the Geneva area, as derived from reflection seismic data. *Eclogae Geologicae Helvetiae*, *88/2*, 235–265.

Sommaruga, A. (1999). Décollement tectonics in the Jura foreland fold-and-thrust belt. *Marine and Petroleum Geology*, *16*(2), 111–134. https://doi.org/10.1016/S0264-8172(98)00068-3

Sonney, R., & Vuataz, F. (2010a). Use of Cl / Br Ratio to Decipher the Origin of Dissolved Mineral Components in Deep Fluids from the Alps Range and Neighbouring Areas. *Ratio*, (April), 25–29.

Sonney, R., & Vuataz, F. D. (2010b). Validation of chemical and isotopic geothermometers from low temperature deep fluids of northern Switzerland. *World Geotermal Congress 2010*.

Vuataz, F. D. (1982). *Hydrogéologie, géochimie et géothermie des eaux thermales de Suisse et des régions limitrophes [Hydrogeological, geochemical and geothermal properties of thermal waters from Switzerland and neighbouring regions]*. Mater Geol. Suisse, Ser. Hydrol. 29.

Vuataz, F. D., & Giroud, N. (2010). *Caractéristiques géochimiques du fluide profond du forage Genève*. SIG Report. Unpublished.

Table 6 - Resuming table reporting the chemical and isotopic compositions of the sampled waters in the Geneva area

Sampling location		Puits Matthieu	Source de la Doua	Source Jules Cesar	GEO-01	Thonex
Date of sampling	**Unit**	11/12/18	11/12/18	11/12/18	12/12/18	12/12/18
Elevation (m a.s.l.)		497	550	401	415	428
Field parameters						
Colour (sensoric)		neutral	neutral	neutral	neutral	neutral
Turbidity (sensoric)		clear	clear	clear	clear, oil streaks	clear
Odour (sensoric)		without	without	without	H2S	H2S, organic
Air temperature	°C	5	4	2	2	-1
pH		7.4	7.2	7.1	7.7	7.7
Electric conductivity	µS/cm	377	446	817	376	1789
Water temperature	°C	8.6	9.5	12.1	32.4	14.6
Oxygen concentration	mg/l	11.1	10.5	7.9	0.1	< 0,1
Redox potential	mV	348	351	386	-103	14
Alkalinity (pH 4.3)	mmol/l	3.8	4.65	5.75	3.5	5.65
Acidity (pH 8.2)	mmol/l	0.19	0.32	0.33	0.07	0.21
Lab parameter						
Physico-chemical parameter						
pH		7.5	7.3	7.3	7.5	7.7
Electric conductivity	µS/cm	379	446	814	378	1842
Alkalinity (pH 4.3)	mmol/l	3.8	4.56	5.74	3.14	5.66
Acidity (pH 8.2)	mmol/l	0.19	0.32	0.33	0.07	0.21
Main anions and cations						
Sodium (Na+)	mg/l	1.2	1.0	30	32	260
Potassium (K+)	mg/l	0.5	0.2	3	2.2	9.6
Calcium (Ca2+)	mg/l	72	91	110	27	60
Magnesium (Mg2+)	mg/l	4.1	2	19	14	30
Ammonium (NH4+)	mg/l	< 0,05	< 0,05	< 0,05	0.18	2.9
Bicarbonate (HCO3-)	mg/l	232	278	350	192	345
Chloride (Cl-)	mg/l	2.2	1.9	60	10	410
Sulfate (SO42-)	mg/l	2.7	2.4	43	19	< 0,2
Nitrate (NO3-)	mg/l	6.7	3.8	17	< 0,2	< 0,2
Nitrite (NO2-)	mg/l	< 0,01	< 0,01	< 0,01	< 0,01	< 0,01
Charge Balance	%	0.3	0.32	2.09	4.54	2.27
Trace elements and metals						
Barium (Ba2+)	mg/l	< 0,02	< 0,02	0.13	0.04	-
Boron (B)	mg/l	< 0,05	< 0,05	< 0,05	0.05	1.6
Bromide (Br-)	mg/l	< 0,1	< 0,1	< 0,1	2.4	5.5
Fluoride (F-)	mg/l	< 0,05	< 0,05	< 0,05	< 0,05	0.5
Jodide (J-)	mg/l	< 0,005	< 0,005	0.005	0.07	0.66
Lithium (Li+)	mg/l	< 0,005	< 0,005	0.005	0.07	0.66
Rubidium (Rb)	mg/l	<0,001	<0,001	<0,001	0.0037	0.034
Cesium (Cs)	mg/l	<0,0001	<0,0001	<0,0001	0.0003	0.005
ortho-Phosphate (PO43-)	mg/l	< 0,03	< 0,03	< 0,03	< 0,03	< 0,03
Selenium	mg/l	< 0,001	< 0,001	< 0,001	< 0,001	< 0,001
Silicium	mg/l	0.65	1.3	4.4	6.6	13.6
Strontium (Sr2+)	mg/l	0.07	0.04	0.29	2.4	6.6
Sulfide tot (HS-, S2-)	mg/l	< 0,1	< 0,1	< 0,1	21.7	< 0,1
Thiosulfate (S2O32-)	mg/l	< 0,5	< 0,5	< 0,5	< 0,5	< 0,5
Aluminium	mg/l	0.011	0.01	< 0,005	0.1	< 0,005
Arsenic	mg/l	< 0,001	< 0,001	< 0,001	< 0,001	< 0,001
Lead	mg/l	< 0,001	< 0,001	< 0,001	< 0,001	< 0,001
Iron tot.	mg/l	< 0,02	< 0,02	< 0,02	< 0,02	2.6
Copper	mg/l	0.004	0.003	0.006	< 0,001	0.005
Manganese tot	mg/l	0.01	< 0,01	< 0,01	< 0,01	0.26
Nickel	mg/l	< 0,001	< 0,001	< 0,001	< 0,001	< 0,001
Uranium	mg/l	0.014	0.0002	0.0005	< 0,0001	< 0,0001
Zinc	mg/l	0.003	0.003	0.005	0.002	0.04
Chromium tot	mg/l	< 0,001	< 0,001	0.001	< 0,001	< 0,001
TIC	mg/l	51.8	66	80.9	40.5	73.7
Isotopes						
d18O-H2O	‰	-10.45	-10.15	-9.54	-11.33	-11.12
d2H-H2O	‰	-72.1	-70.8	-68.6	-78.1	-82
3H-H2O	TU	6,5±0,7	5,3±0,4	6,3±0,6	<0,6	<0,6
d13C-DIC	‰	-14.9	-14.7	-16	-4.4	1.9
14C-TIC	pmC				18,01 ± 0,72	2,24 ± 0,14
SF6	fmol/l	3,70 ± 0,40	3,60 ± 0,40	3,00 ± 0,30	-	-